ELSEVIER

Materials Science and Engineering B88 (2002) 73–78

MATERIALS SCIENCE & ENGINEERING B

www.elsevier.com/locate/mseb

Processing and properties of vanadium doped strontium niobate

Seana Seraji, Yun Wu, Steven Limmer, Tammy Chou, Caroyln Nguyen, Mike Forbess, G.Z. Cao *

Department of Material Science and Engineering, University of Washington, 302M Roberts Hall, P.O. Box 352120, Seattle, WA 98195-2120, USA

Received 4 April 2001; received in revised form 8 October 2001; accepted 10 October 2001

Abstract

Strontium niobate was doped with vanadium and the resulting effects on the dielectric properties of the material were studied. It was shown that the single-phase slab perovskite structure was maintained with up to 10 at.% vanadium doping. Microstructure and dielectric properties of the samples were studied. The average grain size of the samples appeared to increase with increasing vanadium content and dielectric properties were significantly enhanced by the addition of vanadium. It is hypothesized that this is due to the smaller atomic radius of vanadium in comparison to niobium, which results in more 'rattling space' within the oxygen octahedron in the structure of the $Sr_2Nb_2O_7$.

Keywords: Vanadium doping; Dielectric properties; Layered perovskite ferroelectric

1. Introduction

Ferroelectric and piezoelectric materials have many interesting and useful properties that can be used in a wide variety of applications, ranging from the traditional, such as capacitors [1], to the cutting edge, for instance, actuators in micro-electro-mechanical systems (MEMS) [2,3], acoustic tools [4] and non-volatile RAM [5], just to name a few. Many of these applications demand a very stable material that can withstand at least 10^{12} read/write cycles without experiencing significant fatigue effects [5]. Lead zirconate titanate (PZT), among other functional ceramics, has received much attention of late, due to its excellent piezoelectric and ferroelectric properties [2,6–8]. However, this material system has serious limitations. PZT has a relatively low Curie point [1], which effectively limits the temperature to which the material can be exposed. Fatigue is also a major concern with PZT, for it tends to lose much of its 'switching charge' after only 10^6–10^8 cycles [9]. Also, it is a lead-based system, which is not only a hazardous material, but also has a relatively high vapor pressure [5].

Strontium niobate ($Sr_2Nb_2O_7$) is a very promising candidate for such applications because of its high thermal stability (with a very high Curie point of 1342 °C) and resistance to fatigue [7,9,10]. $Sr_2Nb_2O_7$ has an orthorhombic ($a = 3.97$, $b = 26.86$, $c = 5.72$ Å) [10], slab perovskite structure [11]. Each niobium atom is coordinated to six oxygen atoms in an octahedral geometry. Strontium atoms surround these oxygen-niobium octahedral units. The structure is similar to the bismuth layered perovskite structure of materials, which are often represented by $(Bi_2O_2)^{2+}$ $(M_{m-1}\ R_m\ O_{3m+1})$. In these materials, the perovskite cells are packed in between layers of the $(Bi_2O_2)^{2+}$. In strontium niobate however, Sr^{2+} replaces the bismuth layer and the perovskite units are twisted relative to one another at room temperature [12]. Since $Sr_2Nb_2O_7$ is such a promising material for a wide variety of cutting edge applications, a significant amount of research is being carried out with this material system. Grain orientation and electrical properties have been studied by Fukuhara et al. [13]. Novel methods for processing $Sr_2Nb_2O_7$ have also been a wide area of study. Sol-gel processing of thin films of $Sr_2Nb_2O_7$ has been reported [14], as well as rapid thermal annealing [15], molten salt

* Corresponding author. Tel.: +1-206-616-9084; fax: +1-206-543-3100.

E-mail address: gzcao@u.washington.edu (G.Z. Cao).

0921-5107/02/$ - see front matter
PII: S0921-5107(01)00909-6

synthesis [10] and chemical co-precipitation [16]. Fujimori et al. have created ferroelectric field effect transistor devices from $Sr_2Nb_2O_7$-family materials [5,17]. The majority of these reports have been focused on either characterization or processing of $Sr_2Nb_2O_7$ materials. The objective of the current work however, was to improve the dielectric properties of the material through doping with vanadium oxide.

Recently, much work has come out describing the effects of partial cation substitution in dielectric materials [18–21]. It has been reported that partial cation substitution has resulted in lowered processing temperatures and an increased relative density [19]. More importantly, it has been shown that partial substitution has led to enhanced dielectric properties [19–22]. For example, it has been reported that significant improvements in electrical properties were obtained with selective *b*-site substitution in a layered perovskite material system. Significant enhancements in the dielectric properties of SBN ($SrBi_2Nb_2O_9$) were observed after doping with vanadium [19,20]. It was proposed that the improvements were a result of the difference in ionic radius between vanadium and niobium (V^{5+} is $\approx 15\%$ smaller than Nb^{5+}). Since a smaller atom was substituted for the center atom of the oxygen octahedron, the 'rattling space' within the oxygen octahedron [23] was increased. This, in turn, caused a greater polarization, which led to a higher dielectric constant in the material [19]. The goal of this research was to improve the dielectric properties of $Sr_2Nb_2O_7$ by selective *b*-site doping. This was carried out by doping $Sr_2Nb_2O_7$ with vanadium oxide, ranging from 0 to 20 at. wt.%.

2. Experimental procedure

The samples studied were made using standard ceramic processing techniques. The starting chemicals used were $SrCO_3$, Nb_2O_5 and V_2O_5 (All from Aldrich Chemical Co., 99% purity). $Sr_2(V_xNb_{x-1})_2O_7$ pellets, with x ranging from 0 to 0.20 (20 at.%) were studied. The powders were combined in their desired ratios and then ball milled in acetone for over 24 h to homogenize and admix the components. They were subsequently dried, crushed and then fired in air at 900 °C for 2 h to form the desired perovskite phase. Pellets were then pressed from the admixed and fired powders. This was carried out by cold uni-axial pressing at 250 MPa. Approximately 1–2 wt.% polyvinylalcohol (PVA, Aldrich Chemical Co.) was used as a binding agent. The pellets were then sintered in a two-phase firing process. The first step was a low temperature fire (800 °C), the purpose of which was to burn out the organic binder. A second, high-temperature firing step (1200 °C for 1 h) was also carried out in order to further densify the pellets, as well as create a single phase perovskite structure. The phase of each sample was verified by X-ray diffraction (XRD, Philips 1830). Scanning electron microscopy (JEOL, 5200) was used to study the microstructures of the sintered samples.

In order to carry out electrical property measurements, electrodes were put on the pellets. The dielectric constant and loss tangent as functions of temperature up to 630 °C were measured using a Hewlett-Packard Precision LCR Meter 4284A. Unfortunately, the effects of doping on the Curie point of the material could not be studied at the time of this publication. The Curie point of $Sr_2Nb_2O_7$ is 1342 °C and the high temperature testing equipment necessary to carry out such experiments was not available. The effects of vanadium doping on the poling properties of strontium niobate were also studied. The $Sr_2Nb_2O_7$ samples created were polycrystalline ceramics. After processing, the crystal axes of the grains were randomly oriented. The sample was then subjected to a static electrical field, which may have resulted in the alignment of the polar axes of the material [1]. However, as with any poling process, it is unlikely that complete axes alignment occurred (while the 180° switching can be almost complete, switching through other angles can often limit polarization [1]). Various potentials (ranging from 0 to 50 kV cm^{-2}) were used to pole the samples. The samples were allowed to age before measuring dielectric properties.

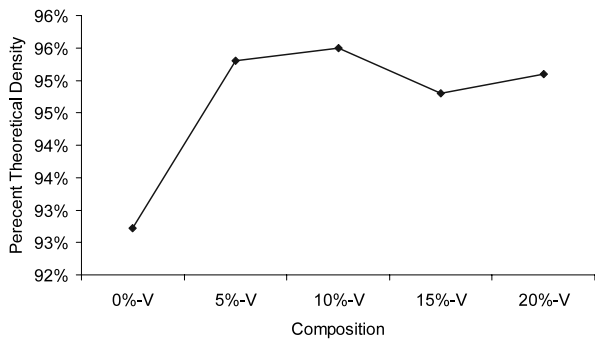

Fig. 1. Densities of strontium niobate pellet as a function of vanadium doping content.

3. Results and discussions

3.1. Densification and formation of $Sr_2(Nb,V)_2O_7$

All of the pellets achieved at least 92% theoretical density. No significant weight loss occurred beyond the loss of the organic binders. It appears that the addition of vanadium improves the densification process because pellets doped with vanadium in general achieved higher densities ($\approx 96\%$ theoretical density) than the un-doped $Sr_2Nb_2O_7$, as can be seen in Fig. 1. The addition of vanadia into the system may promote the formation of

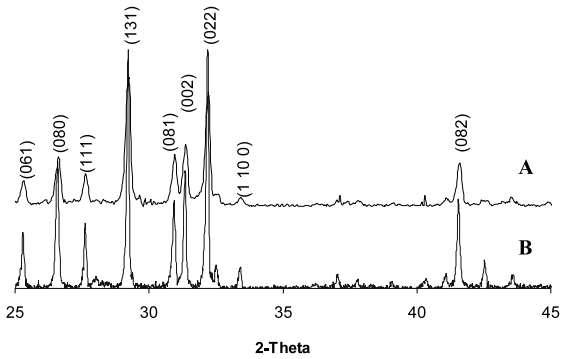

Fig. 2. XRD spectra of the (A) 10%-V strontium niobate sample compared to (B) an undoped $SR_2NB_2O_7$ after a two-step sintering process, showing a single phase with the desired slab perovskite structure.

oxide liquid during the sintering, partly due to the low melting temperature of the vanadia (690 °C; [19]). Similar enhancements in sintering and higher densification were seen with vanadium doping in SBN ($SrBi_2Nb_2O_9$) ferroelectrics [19,20]. Wu et al. also performed exhaustive experiments on the effects of vanadium doping on formation temperature [19].

Fig. 2 is the indexed XRD spectra from an undoped and 10%-vanadium doped strontium niobate samples. The two identical spectra suggest that a single-phase perovskite structure was achieved with vanadium doping, with no appreciable secondary phases. Further experiments revealed that a layered perovskite phase is maintained only at low vanadium concentrations (< 20 at.% V). Crystallinity degradation, as well as the formation of other phases, was seen at higher vanadium doping concentrations. As a result, no further experiments were carried out with the 20%-V samples. These results were expected, for crystallographic arguments indicate that a stable perovskite is unattainable with full vanadium substitutions, according to the R_{cation}/R_{anion} ratio calculations [24].

3.2. Microstructure

In Fig. 3(A–D) are SEM micrographs of fracture surfaces of the $Sr_2Nb_2O_7$ samples with 0, 5, 10 and 15 at.% vanadium, respectively. All samples appear to be relatively dense, although some pores and voids were seen. Another trend observed from the micrographs deal with grain size. In general, the grain size of the ceramic samples was seen to increase with vanadium content. This may indicate that the incorporation of vanadium into the $Sr_2Nb_2O_7$ promotes grain growth and densification. This was surprising, for alternate cation substitutions in isotropic perovskite ferroelectrics often lead to decreased cross-grain boundary diffusion during sintering, which would result in smaller grains at higher doping levels [1]. Increased grain size may be attributed to the presence of oxide liquid phase during sintering in the vanadia doped $Sr_2Nb_2O_7$ samples. The liquid phase would significantly enhance the densifica-

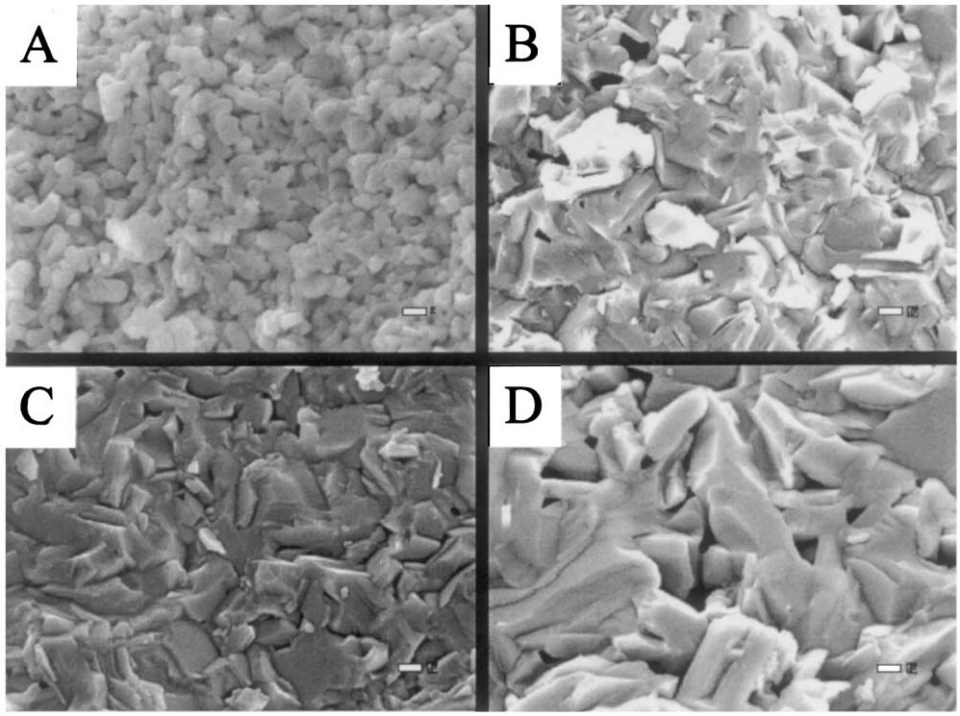

Fig. 3. SEM micrographs of fracture surfaces of strontium niobate samples, clockwise from top left, (A) No doping; (B) 5% V; (C) 10% V; (D) 15% V (scale bar = 1 micron).

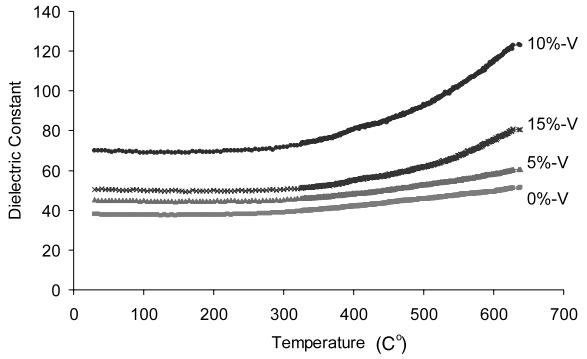

Fig. 4. Dielectric constant as a function of temperature for various strontium niobate compositions measured at 100 kHz.

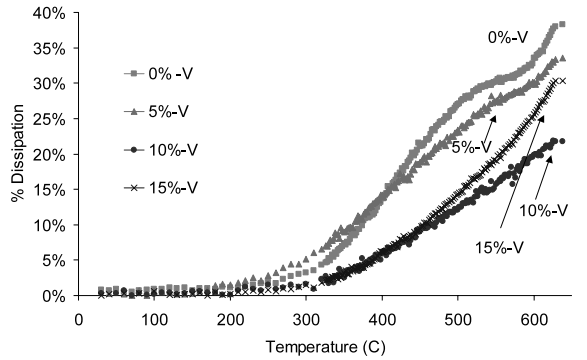

Fig. 5. Chart of tangent loss as a function of temperature for the various compositions of strontium niobate samples (measured at 100 kHz).

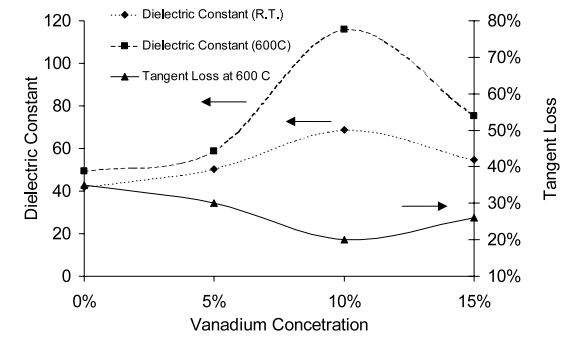

Fig. 6. Summary chart of dielectric constant (at room temperature as well as 600 °C) and tangent loss at 600 °C as a function of vanadium concentration, showing the significant enhancement of dielectric properties of the 10%-V sample.

tion and grain growth through a dissolution–reprecipitation process. This increase in grain size with vanadium content was also observed in the $SrBi_2(V_xNb_{1-x})_2O_9$ system [19]. It was also noticed that the non-doped $Sr_2Nb_2O_7$ exhibited intergranular fracture, however, doped $Sr_2Nb_2O_7$ samples exhibited at least partial transgranular fracture. This may be due to the fact that the vanadium doping improves the packing of the grains and increases the grain size.

3.3. Dielectric properties

The dielectric properties of the $Sr_2Nb_2O_7$ doped with various amounts of vanadia were studied. It was found that the addition of vanadia resulted in an appreciable enhancement in dielectric constant over a wide range of temperatures. The results also indicate that the optimum vanadium doping level is somewhere around 10 at.%. Fig. 4 is a chart of dielectric constant versus temperature for $Sr_2(Nb,V)_2O_7$ at various vanadium doping levels. One can see that an increase in vanadium level was commensurate with an increase in dielectric constant values for samples up to 10 at.% vanadium. Degradation in dielectric constant was seen at higher vanadium doping levels. This is thought to be a result of the degradation of the slab perovskite structure at the higher vanadium concentrations.

The dielectric constant values at room temperature were found to be in line with other reported room temperature dielectric constant values, which range anywhere from the low 40s up to 75, depending on the orientation and the processing of the sample [5,13]. Fig. 5 shows the tangent loss as a function of temperature for the $Sr_2Nb_2O_7$ with various doping levels. The tangent loss for all samples increased rapidly at temperatures >300 °C. This high tangent loss may be attributed to an increased vacancy related dielectric relaxation at high temperatures. It was also found that the sample with the 10% vanadium doping performed the best, with the lowest dissipation. It is interesting to note that the dissipation of the 10% sample was almost half that of the undoped $Sr_2Nb_2O_7$ sample. Reduction in tangent loss with vanadium doping was also found in SBN ferroelectrics [20].

Fig. 6 summarizes the dielectric constants at room temperature and 600 °C and tangent loss at 600 °C as a function of vanadia doping concentration (all measured at 100 kHz). This figure illustrates the trends seen throughout the experiments, particularly that the 10% sample consistently outperformed all of the other samples.

3.4. Poling effects

The samples were poled at various voltages for various lengths of time and the dielectric constants were measured before and after poling. $Sr_2Nb_2O_7$ samples were poled for 30, 60 and 95 min under an electric field of 35 kV cm^{-1} field. This voltage is nearly six times the coercive field for $Sr_2Nb_2O_7$ (6 kV cm^{-1}) [5]. Fig. 7 shows the effects of the various durations of poling time on the dielectric constant and demonstrates that the poling resulted in an increase in dielectric constants. The total difference is $\approx 9\%$. It is well known that poling an isotropic perovskite ferroelectric material increases its dielectric constant [18]. It is believed that this

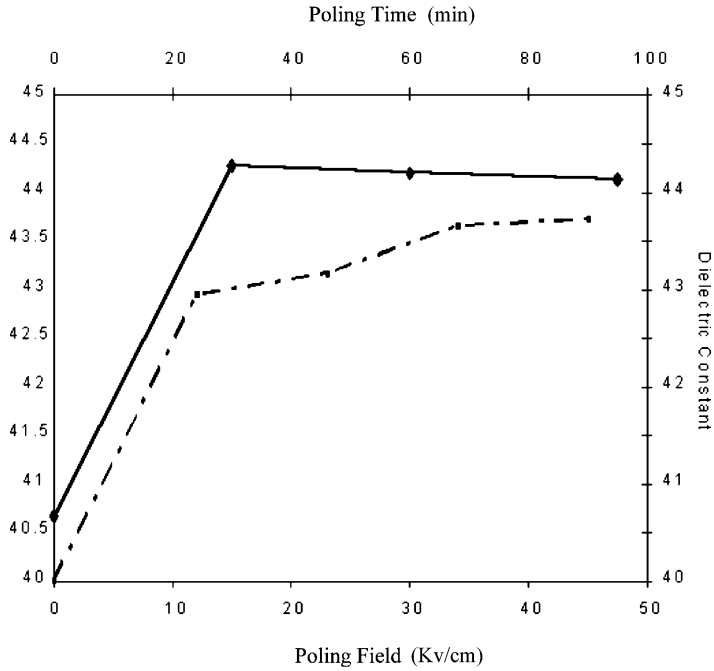

Fig. 7. Chart of dielectric constant as a function of poling time and field for undoped $Sr_2Nb_2O_7$ measured at 100 kHz.

is due to the reorientation of the domains in the material [18]. For an orthorhombic ferroelectric, the domains or dipoles will align in the direction of the poling field. It is very likely that along the *c*-axis or dipolar direction, there is more space for ions to polarize, particularly the body-centered ions (Nb^{5+} and V^{5+}) inside the elongated oxygen octahedra, so that a higher dielectric constant would be obtained. As can be seen, the difference between the different poling times was actually quite small. We believe that this is a saturation effect. For a given voltage, only so many axes can be aligned and thus, after all of the domains that will align have been aligned, longer durations will not result in more polarization. In fact, as the duration of time increased, a slight degradation in capacitance was seen. This may have been due to a build up of internal stresses within the samples as a result of the high voltages. These results indicated that 30 min would be an appropriate length of time to pole the samples.

A series of experiments were carried out at 12, 23, 34 and 45 kV cm^{-1} and the dielectric constant was measured before and after poling. Samples poled at fields higher than 45 kV cm^{-1} could not be tested reliably, for dielectric breakdown was often encountered. Fig. 7 displays these results as well. From the chart, a significant increase in dielectric constant can be seen between the pre-poling sample and the sample poled with a 12 kV cm^{-1} electric field. Much smaller increases were observed for incrementally increasing electric fields above 12 kV cm^{-1}. These results indicate that an electric field of 12 kV cm^{-1} is sufficient to align the domains or dipoles in $Sr_2Nb_2O_7$. It is interesting to note that the difference between the highest and lowest capacitance values for this test was $\approx 9.3\%$. From the above results, it was determined that 40 kV cm^{-1} would be a sufficient poling electric field.

The poling behavior of the 10 at.% V doped $Sr_2Nb_2O_7$ samples were also studied. This composition was chosen because it outperformed the other samples in the previously described dielectric constant experiments. After much experimentation with poling parameters with the undoped samples, we found that a field of 40 kV cm^{-1} for 30 min consistently yielded poled samples. Therefore, these empirically optimized conditions were used to pole the 10 at.% V samples as well. The results of these experiments can be seen in Fig. 8 and Table 1. From the data, it is apparent that

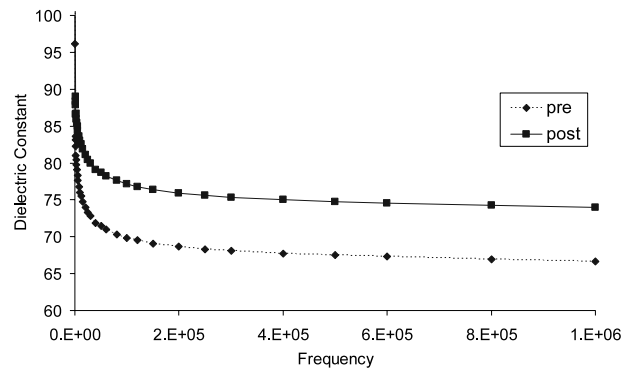

Fig. 8. Chart of dielectric constant as a function of frequency for a 10 at.% $Sr_2Nb_2O_7$, pre- and post-poling. Poling was carried out at 40 kV cm^{-1} for 30 min.

Table 1
Summary of poling effects on $Sr_2Nb_2O_7$ and $Sr_2Nb_2O_7$ with 10 at.% vanadia, all measurements at 100 kHz

Samples	Dielectric constant		Tangent loss	
	Pre-poling	Post-poling	Pre-poling	Post-poling
Strontium niobate	39.0	43.3	0.0885	0.0046
Strontium niobate with 10 at.% V	66.1	74.2	0.0508	0.0447

the poling has the same influences on the dielectric properties of both $Sr_2Nb_2O_7$ and $Sr_2Nb_{1.8}V_{0.2}O_7$ samples. Poling resulted in an increase in dielectric constant and a decrease in tangent loss.

One possible explanation for this decrease in tangent loss is that non-180° domains are more difficult to switch and thus require more energy to switch, which contributes to the tangent loss. However, after poling, there are less non-180° domains as a result of the applied field. Therefore, when exposed to a switching field, more domains are already aligned into the 180° direction and therefore, less energy is lost due to non-180° domain switching. Another point of interest is that the overall difference in dielectric constants between the poled and unpoled samples was greater for the doped than the undoped samples ($\approx 9\%$ for the undoped $Sr_2Nb_2O_7$ and $\approx 13.5\%$ increase for the 10%-V). One explanation is that perhaps the vanadium doping not only allows a greater degree of polarization in the unit cell, but also enhances the poling effects in the $Sr_2Nb_2O_7$, allowing more room for the center ions to move.

4. Conclusions

The samples were found to have from 92 to 96% theoretical density and that the incorporation of vanadia appeared to enhance the densification process. The resulting pellets were verified to be single-phase $Sr_2Nb_2O_7$ by XRD. From the XRD analysis, it was found that the perovskite structure was maintained up to 15 at.% vanadia. At higher doping concentrations, secondary phases developed. From the SEM work, it was observed that the vanadium doping seemed to result in increased grain size and transgranular fracture occurred in doped samples. The dielectric constant increased with vanadium doping up to 10 at.%, after which it decreased. This was thought to be a result of the increased 'rattling space' due to the smaller size of the niobium atom with respect to niobium. The doping also appeared to enhance the poling properties of the $Sr_2Nb_2O_7$.

Acknowledgements

The authors would like to thank PNNL (S. Limmer) Ford Motor Co. (S. Seraji) and the Center for Nanotechnology at the University of Washington (Y. Wu, S. Limmer, S. Seraji) for financial support.

References

[1] A.J. Moulson, J.M. Herbert, Electroceramics, Chapman and Hill, London, 1990.
[2] K. Brooks, D. Damjanovic, A. Kholkin, I. Reaney, N. Setter, et al., Integr. Ferroelec. 8 (1995) 13.
[3] D. Polla, L. Francis, Annu. Rev. Mater. Sci. 28 (1998) 563.
[4] G. Yi, M. Sayer, Ceramic Bulletin, vol. 70, seventh ed, 1991, p. 1173.
[5] Y. Fujimori, N. Izumi, T. Nakamura, A. Kamisawa, Jap. J. Appl. Phys. 37 (9) (1998) 5207.
[6] E. Cattan, T. Haccart, D. Remiens, J. Appl. Phys. 86 (12) (1999) 7017.
[7] S.M. Zanetti, E.B. Araujo, E.R. Leite, E. Longo, J.A. Varela, Mater. Letts. 40 (1999) 33.
[8] K. Watanabe, E. Sumitomo, K. Katori, H. Yagi, J.F. Scott, Appl. Phys. Letts. 73 (1) (1998) 126.
[9] H. Watanabe, T. Mihara, Jap. J. Appl. Phys. 34 (1) (1995) 5240.
[10] B. Brahmaroutu, G.L. Messing, S.T. Trolier, McKinstry, J. Am. Ceram. Soc. 82 (6) (1999) 1565.
[11] N. Ishizawa, F. Marumo, Acta Cryst. B31 (1975) 1912.
[12] K. Okuwada, S. Nakamura, H. Nozawa, J. Mater. Res. 14 (1999) 855.
[13] M. Fukuhara, C.-Y. Huang, A. Bhalla, R. Newnham, J. Mater. Sci. 26 (1991) 61.
[14] A. Prasadarao, U. Selvaraj, S. Komareneni, J. Mater. Res. 10 (3) (1995) 704.
[15] M. Shoyama, A. Tsuzuki, K. Kato, N. Murayama, Appl. Phys. Letts. 75 (4) (1999) 561.
[16] H.D. Nam, I.H. Park, Y.J. Song, S.B. Desu, Ferroelectrics 186 (1996) 137.
[17] Y. Fugimori, N. Izumi, T. Nakamura, A. Kamisawa, Y. Shigematsu, Jpn. J. Appl. Phys. 36 (9) (1997) 5935.
[18] V. Koval, J. Briancin, Ferroelectrics 193 (1997) 41.
[19] Y. Wu, G.Z. Cao, Appl. Phys. Letts. 75 (1999) 2650.
[20] Y. Wu, G.Z. Cao, J. Mater. Res. 15 (7) (2000) 1583.
[21] M.J. Forbess, S. Seraji, Y. Wu, C. Nguyen, G.Z. Cao, Appl. Phys. Letts. 76 (2000) 2934.
[22] P. Duran Martin, A. Castro, P. Millan, B. Jimmenez, J. Mater. Res. 13 (1998) 2565.
[23] B.D. Culity, Elements of X-Ray Diffraction, Addison-Wesley, Reading, MA, 1956.
[24] W. Callister Jr, Materials Science Engineering, an Introduction, fifth ed, Wiley, New York, 2000.